

Return Loss Optimization in Rectangular Microstrip Patch Antennas Using Response Surface Methodology (RSM) for 5G Applications

Bich Ngoc Tran-Thi^{1,*}, Dang Van Su²

¹Vietnam Aviation Academy, Ho Chi Minh City, Vietnam; ngocttb@vaa.edu.vn

²Ho Chi Minh City University of Industry and Trade, Ho Chi Minh City, Vietnam; sudv@huit.edu.vn

Abstract

In recent decades, wireless communication has advanced significantly. People increasingly rely on the Internet of Things, cloud computing, and big data analytics. These services require higher data rates, faster transmission and reception times, greater coverage, and increased throughput. 5G technology supports all of these features. Antennas, essential components of modern wireless devices, must be designed to meet the growing demand for fast and intelligent products. This study aims to optimize the dimensions and characteristics of a rectangular patch antenna. To examine the impact of independent variables (such as patch length, patch width, inset slot length, and inset slot width) on the response variables (return loss and resonant frequency), Response Surface Methodology (RSM) combined with Central Composite Design (CCD) was applied. The findings of the RSM analysis indicated that the experimental data were best represented by a quadratic polynomial model, with regression coefficients exceeding 0.970 for all responses. The optimized parameters identified are as follows: a patch length of 4.7 mm, a patch width of 4.7 mm, an inset slot length of 0.8 mm, and an inset slot width of 1.0 mm. The antenna designed using these optimized parameters achieved a target return loss of -45.865 dB at a frequency of 28.122 GHz. Finally, the results were validated using CST Studio Suite, which demonstrated good agreement with the experimental data.

Received on 21 March 2025; accepted on 05 June 2025; published on 12 June 2025

Keywords: 5G, Central Composite Design (CCD), patch antenna, return loss, Response Surface Methodology (RSM).

Copyright © 2025 Bich Ngoc Tran-Thi *et al.*, licensed to EAI. This is an open access article distributed under the terms of the [CC BY-NC-SA 4.0](#), which permits copying, redistributing, remixing, transformation, and building upon the material in any medium so long as the original work is properly cited.

doi:10.4108/eetinis.v12i3.8948

1. Introduction

Wireless systems have experienced significant advancements over the years. The antenna is central to every wireless communication system, a crucial element that facilitates the transmission and reception of data via electromagnetic waves. With the continuous evolution of communication technology, the adoption and utilization of wireless devices have expanded considerably. Consequently, future generations of wireless communication systems are expected to offer even higher data rates and enhanced capacities, with the antenna remaining an indispensable component for efficient data exchange. Microstrip patch antennas play a vital

role in wireless communication. They consist of a dielectric substrate, a ground plane, and a thin metallic patch usually made of copper or gold. The patch is separated from the ground plane by the dielectric substrate. Commonly called "patch antennas," they are well-known for their flat and compact design [1–3]. These antennas generally consist of a metallic patch or conductor printed on a dielectric substrate and may include a ground plane depending on the design [4]. Patch antennas come in various shapes, including circular, rectangular, square, elliptical, triangular, and dipole designs. Circular and rectangular microstrip antennas are the most widely used, especially in developing 5G applications [4]. These antennas operate by transmitting and receiving information through radio waves. Microstrip patch antennas offer advantages over

*Corresponding author. Email: ngocttb@vaa.edu.vn

traditional antennas, such as being lightweight, cost-effective, foldable, and easy to manufacture. They support multiple frequency operations and often outperform conventional antennas in terms of efficiency and versatility. Consequently, they are extensively used in telecommunications, including mobile phones, defense systems, and wireless wearable devices. Despite their many benefits, microstrip antennas face limitations, such as narrow bandwidth and low radiation efficiency [4].

Antenna design is inherently a multi-objective challenge, requiring the simultaneous consideration of several often conflicting criteria. While the primary focus is typically on optimizing reflection [5], other critical factors include gain [6, 7], radiation pattern [8], and size, which is particularly important for specific applications [9, 10]. Despite this complexity, most antenna design problems are treated as single-objective tasks in the optimization field. Typically, only one objective—most commonly the reflection characteristics—is directly optimized, while other criteria are managed through the use of constraints or penalty functions [10]. To increase the efficiency of antenna design, extensive research has been conducted on antenna synthesis and design optimization. Patch antennas can be tailored to function across a wide frequency spectrum, ranging from microwave to millimeter-wave bands, by simply adjusting their physical dimensions. This flexibility enables them to accommodate the varying frequency requirements of numerous wireless standards and applications [11]. Additionally, their fabrication benefits from well-established Printed Circuit Board (PCB) manufacturing techniques, ensuring a cost-efficient and scalable production process [12, 13]. In [14], the authors introduced a patch antenna design method utilizing two evolutionary optimization techniques: Central Force Optimization (CFO) and Differential Evolution (DE). CFO is a recently developed deterministic evolutionary algorithm (EA) inspired by gravitational kinematics, while DE is a population-based evolutionary optimization algorithm that relies on mutation and crossover operations. These optimization methods offer a powerful approach to antenna design, allowing engineers to achieve specific performance criteria without relying on a labor-intensive trial-and-error process.

The Design of Experiments (DoE) method is a structured, statistical approach used to identify the relationships between factors that influence a process and the resulting output [15]. Response Surface Methodology (RSM) is design technique for modeling that aims to optimize the levels of independent variables. The RSM is a subset of DoE that focuses on modeling and optimizing a response affected by multiple variables. A widely used design within RSM generates data to build accurate quadratic models.

Designing a patch antenna requires defining its geometric parameters, including the patch dimensions and feed position, to achieve an optimal configuration that satisfies specific performance criteria. A trial-and-error approach alone can be inefficient and may not lead to the best possible design. Therefore, utilizing advanced optimization techniques enables designers to develop high-performance antennas more efficiently and effectively. The RSM optimizes the design of patch antennas by minimizing the need for extensive simulations and experiments. This objective is achieved through structured experimental designs, such as Central Composite Design (CCD) and Box-Behnken Design (BBD), among others. In this study, we specifically select CCD. As a key method in RSM, CCD is the most popular class of designs needed for fitting a second-order (quadratic) model. This second-order polynomial model effectively captures nonlinear interactions between variables, thereby enhancing performance optimization while reducing computational costs. Additionally, the RSM helps identify the optimal configurations to maximize bandwidth and minimize return loss, making it a valuable tool for improving antenna efficiency in wireless communication and radar applications.

The authors in [16] explore the integration of DoE and RSM to optimize the performance of microstrip patch antennas. Their approach is shown to be more efficient than traditional electromagnetic simulation methods. Meanwhile, to enhance impedance bandwidth and operational frequencies for 5G applications, RSM is utilized to optimize the geometric parameters of a pi-slotted rectangular microstrip patch antenna [9]. Additionally, the authors in [17] examined the use of RSM to assess the impact of design factors on antenna responses, which aids in optimizing a multiband reconfigurable antenna. Furthermore, another study applies RSM to predict the performance characteristics of a double elliptical microstrip patch antenna designed for radiolocation systems [18]. This method enables accurate predictions of critical parameters such as bandwidth, gain, and radiation patterns.

This study presents a DoE approach, specifically CCD-RSM, to enhance the efficiency of antenna optimization. The key layout parameters of the patch antenna are analyzed using RSM to optimize its return loss at resonant frequency of 28 GHz band. The results demonstrate that employing DoE to estimate and enhance antenna performance is more effective than relying solely on computer simulation technology (CST) simulation tools. An antenna optimized through the DoE method was tested, and the simulated results showed a directivity of 5.58 dBi and a return loss of -45.865 at a resonant frequency of 28.122 GHz.

This paper is organized as follows: Section 2 and Section 3 provide a comprehensive overview of the

structure and methods employed in the antenna design. 4 presents the simulation results and examines their implications. Finally, Section 5 summarizes the main conclusions drawn from the study.

2. Antenna Structure

The efficiency of a microstrip patch antenna is mainly affected by its geometric configuration, structural dimensions, and the material properties used in its construction. In this study, a rectangular patch was chosen because it is easy to fabricate and analyze. Furthermore, its broader shape offers a wider impedance bandwidth compared to other types of antennas, which improves overall performance. The preliminary design parameters of the radiating element feature a rectangular patch, with its physical dimensions (length and width) determined using the transmission-line model antenna design equations [4, 19]. Fig. 1 illustrates the geometric configuration of the rectangular microstrip patch antenna. The proposed antenna consists of a rectangular radiating patch element with two insets, a ground plane, a substrate, and a feeding component. The radiating element and ground plane, represented as Perfect Electric Conductors (PECs), are positioned on the top and bottom sides of the substrate, respectively. Moreover, FR-4 has been selected as a dielectric substrate material having a thickness of 0.2 mm, dielectric constant (ϵ_r) of 4.3, and tangent loss of 0.0009. A radiating copper metal thickness of 0.02 mm to function at 28 GHz center frequency has been used.

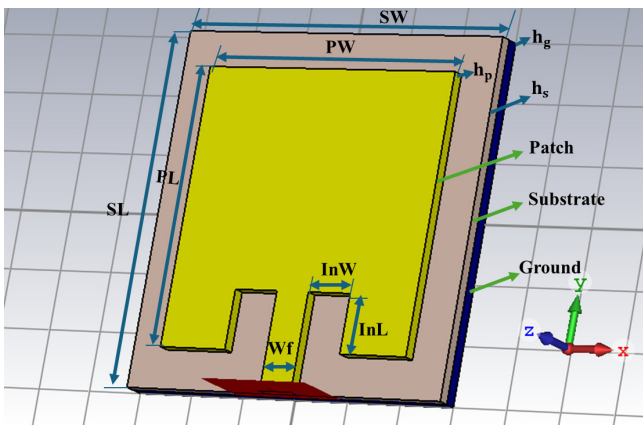


Figure 1. The physical configuration of the projected rectangular microstrip antenna.

The model also incorporates a waveguide port for excitation. The dimensions of the microstrip feed line are calculated using the formula in [4, 19]. The original rectangular patch is modified by inserting slots, which are etched to enhance return loss and improve antenna radiation characteristics. In this paper, the primary

goal is to minimize the reflection coefficient at the 28 GHz band. This focus allows for further parametric studies and optimizations aimed at enhancing the antenna's return loss performance. To simplify, the list of notations used throughout this paper is presented in Table 1.

Table 1. The compilation of symbols and their definitions

Notation	Meaning	Notation	Meaning
h_g	Ground thickness	PL	Patch length
SW	Substrate width	h_p	Patch thickness
SL	Substrate length	Wf	Feedline width
h_s	Substrate thickness	InL	Inset slot length
PW	Patch width	InW	Inset slot width

3. Design of Experiments

Patch antennas require careful tuning of various parameters to achieve desired performance metrics, including return loss, gain, bandwidth, efficiency and radiation pattern. RSM is a statistical and mathematical tool for the systematic modeling and optimization of complicated systems. It facilitates the study of the design area by establishing correlations between design parameters (for example, substrate thickness, patch dimensions, and feed position) and performance responses.

Initially, key variables that influence the system are identified, including patch width, patch length, inset slot width, and inset slot length. Suitable initial values are then selected for the experiment. The main effects and lower-order interactions typically influence the responses, making a two-factor interaction model appropriate for this analysis. The Rotatable CCD-RSM is utilized, focusing on four key independent variables that significantly impact the experimental outcomes. The corresponding performance measures, referred to as responses, are then analyzed.

The objective of this study is to minimize the return loss value (Y) at a specific 28 GHz frequency band. Patch length (A), patch width (B), inset slot length (C), and inset slot width (D) were chosen as independent variables to optimize the circumstances for attaining the lowest return loss value since they have a substantial influence on the outcomes. Under the condition that other parameters of the patch antenna are fixed: $h_g = h_s = h_p = 0.2$ mm, $SW = SL = 6$ mm, $Wf = 0.6$ mm.

The total number of experiments conducted was determined by the formula $N = 2^k + n_c + 2k$, where k represents the number of independent variables, n_c is center point experiments and $2k$ denotes the additional experiments at the star points [15, 20]. In this work, $k = 4$; $n_c = 5$. Thus, a total of $N = 29$ experiments were performed with 16 factorial design experiments,

along with 5 center point experiments to evaluate the error, and 8 additional experiments at the star points, located at a distance of $\alpha = (2^k)^{1/4} = 2$ from the center experimental point. This information is summarized in Table 2.

Table 2. Independent variables and their corresponding levels

Independent variable	Symbol	Coded levels				
		$-\alpha$	-1	0	+1	$+\alpha$
Patch length	X1	4.5	4.6	4.7	4.8	4.9
Patch width	X2	4.5	4.6	4.7	4.8	4.9
Inset slot length	X3	0.7	0.75	0.8	0.85	0.9
Inset slot width	X4	0.9	0.95	1	1.05	1.1

The experimental design centers on the following parameters: a patch length (PL) of 4.7 mm, a patch width (PW) of 4.7 mm, an inset slot length (InL) of 0.8 mm, and an inset slot width (InW) of 1 mm. Based on the preliminary analysis of these parameters, the return loss and resonant frequency are anticipated to exhibit optimal performance characteristics, aligning with expected values.

Table 3. CCD design of experiments.

Std	Run	A:PL (mm)	B:PW (mm)	C:InL (mm)	D:InW (mm)
1	25	4.6	4.6	0.75	0.95
2	18	4.8	4.6	0.75	0.95
3	11	4.6	4.8	0.75	0.95
4	5	4.8	4.8	0.75	0.95
5	24	4.6	4.6	0.85	0.95
6	29	4.8	4.6	0.85	0.95
7	17	4.6	4.8	0.85	0.95
8	21	4.8	4.8	0.85	0.95
9	6	4.6	4.6	0.75	1.05
10	1	4.8	4.6	0.75	1.05
11	26	4.6	4.8	0.75	1.05
12	14	4.8	4.8	0.75	1.05
13	22	4.6	4.6	0.85	1.05
14	7	4.8	4.6	0.85	1.05
15	3	4.6	4.8	0.85	1.05
16	12	4.8	4.8	0.85	1.05
17	23	4.5	4.7	0.8	1
18	27	4.9	4.7	0.8	1
19	28	4.7	4.5	0.8	1
20	16	4.7	4.9	0.8	1
21	10	4.7	4.7	0.7	1
22	15	4.7	4.7	0.9	1
23	19	4.7	4.7	0.8	0.9
24	20	4.7	4.7	0.8	1.1
25	2	4.7	4.7	0.8	1
26	8	4.7	4.7	0.8	1
27	4	4.7	4.7	0.8	1
28	9	4.7	4.7	0.8	1
29	13	4.7	4.7	0.8	1

In this regard, the DoE method is used to perform statistical analysis to obtain the response-surface model, which relates coded variables and can be used experimentally to obtain the responses.

The model used to predict the value of the objective function (Y) is expressed as follows [15]:

$$Y = \beta_0 + \sum_{i=1}^k \beta_i x_i + \sum_{i=1}^k \beta_{ii} x_i^2 + \sum_{i<j}^k \sum \beta_{ij} x_i x_j + \epsilon \quad (1)$$

where x_j and x_i are design or independent variables (e.g., patch length, patch width, inset slot length, inset slot width). β_0 is constant or model coefficient, β_i , β_{ii} and β_{ij} are coefficients for the linear, quadratic, and interaction effects, respectively. k is the number of independent variables and ϵ is the model error [15].

Design-Expert software was used to execute the experimental design using RSM. To obtain the response values, such as return loss (RL) and resonant frequency (F), CST Studio Suite 2018 software is used for simulation with the antenna dimensions specified in Table 3. To minimize potential errors related to the simulation and experimental procedures, the sequence of experimental runs is determined randomly.

The model's fitness is evaluated using results from Analysis of Variance (ANOVA) and residual analysis. These analyses apply model adjustments that improve convergence speed and accuracy. After creating a well-fitted model, parameters are tuned using a limited numerical technique to obtain the required performance. Finally, simulations with the electromagnetic solver CST Studio Suite 2018 confirm the enhanced antenna's performance.

4. Results and Discussion

4.1. CCD-RSM experimental model utilizing Design Expert software

The ANOVA results in Tables 4 and 5 show that quadratic models accurately represented the experimental data. They were also evident that the factors significantly influenced the objective function. A smaller p-value and a larger F-value indicate a highly significant effect of any term on the response variable.

The model F-values of 53.91 (for return loss) and 2863.01 (for resonant frequency) indicate that the models are significant, with only a 5% chance that such large F-values could result from random error. Additionally, p-values of less than 0.05 confirm the models' significance. Specifically, the factors had a significant influence on the models. In contrast, factors with p-values greater than 0.05 do not significantly impact the models. The F-values of 4.94 (for return loss) and 0.8142 (for resonant frequency) demonstrated that the Lacks of Fit are suitable and did not significantly

Table 4. ANOVA analysis of the variables affecting the return loss function

Source	Sum of Squares	df	Mean Square	F-value	p-value	
Model	2641.91	12	220.16	53.91	< 0.0001	significant
A-PL	1.74	1	1.74	0.4258	0.5233	
B-PW	11.40	1	11.40	2.79	0.1143	
C-InL	3.59	1	3.59	0.8783	0.3626	
D-InW	16.17	1	16.17	3.96	0.0640	
AB	58.62	1	58.62	14.35	0.0016	
AC	155.43	1	155.43	38.06	< 0.0001	
BD	160.76	1	160.76	39.36	< 0.0001	
CD	21.54	1	21.54	5.28	0.0355	
A ²	922.85	1	922.85	225.98	< 0.0001	
B ²	934.57	1	934.57	228.85	< 0.0001	
C ²	820.08	1	820.08	200.81	< 0.0001	
D ²	786.56	1	786.56	192.60	< 0.0001	
Residual	65.34	16	4.08			
Lack of Fit	61.21	12	5.10	4.94	0.0679	not significant
Pure Error	4.13	4	1.03			
Cor Total	2707.25	28				

Table 5. ANOVA analysis of the variables affecting the frequency function

Source	Sum of Squares	df	Mean Square	F-value	p-value	
Model	3.78	9	0.4197	2863.01	< 0.0001	significant
A-PL	0.4483	1	0.4483	3057.76	< 0.0001	
B-PW	3.14	1	3.14	21413.87	< 0.0001	
C-InL	0.1014	1	0.1014	691.68	< 0.0001	
D-InW	0.0726	1	0.0726	495.23	< 0.0001	
AB	0.0081	1	0.0081	55.25	< 0.0001	
AD	0.0025	1	0.0025	17.05	0.0006	
BD	0.0009	1	0.0009	6.14	0.0228	
A ²	0.0031	1	0.0031	21.44	0.0002	
B ²	0.0018	1	0.0018	12.57	0.0022	
Residual	0.0028	19	0.0001			
Lack of Fit	0.0021	15	0.0001	0.8142	0.6595	not significant
Pure Error	0.0007	4	0.0002			
Cor Total	3.78	28				

influence the models when compared to pure errors, indicating the models' statistical accuracy [15].

To evaluate the models' predictive performance, we used the optimized return loss and frequency parameters, which were validated by simulating return loss and frequency under optimized conditions.

The regression coded equations for each response variable, formulated using response surface methodology, are detailed below.

$$\begin{aligned}
 RL = & -44.8516 - 0.269167A + 0.689083B \\
 & - 0.386583C - 0.820917D - 1.91413AB \\
 & + 3.11675AC - 3.16975BD + 1.16037CD \\
 & + 5.96392A^2 + 6.00167B^2 \\
 & + 5.62205C^2 + 5.50592D^2
 \end{aligned} \quad (2)$$

$$\begin{aligned}
 F = & 28.1285 - 0.136667A - 0.361667B \\
 & - 0.065C - 0.055D + 0.0225AB + 0.0125AD \\
 & - 0.0075BD - 0.0106705A^2 - 0.00817045B^2
 \end{aligned} \quad (3)$$

ANOVA results revealed that the experimental data could be represented well with a quadratic polynomial model with a coefficient of determination (R^2) values for return loss (RL), and resonating frequency (F) being 0.9759 and 0.9993, respectively. If the value of R^2 is close to one, it indicates a better fit of the model to the actual data. Conversely, lower values of R^2 suggest that the response variables are not suitable for explaining the variation in behavior [15].

4.2. Response surface analysis

Figures 2a, 2b, and 2c illustrate the response surface and contour plots depicting the interactions between variables affecting return loss (RL). Specifically, they show RL as a function of PW and PL, InW and PL, and InL and PL, respectively. The plots exhibit a noticeable curvature, highlighting the effectiveness of the models used [15, 21]. Meanwhile, Figures 2d, 2e, and 2f present 3D response surface plots for resonant frequency (F), showing F as a function of PW and PL, InL and PL, and InW and PL. These plots display a nearly flat curvature, indicating a more stable frequency response.

In the contour plots shown in Fig. 2, the dark regions represent lower response values, while the light-colored regions indicate higher response values.

The contour plots display lines of constant response, each representing a specific value. Each contour line indicates a particular height on the response surface. The features observed in the response plots suggest that the proposed models are both appropriate and effective. In the surfaces of "PL versus PW, PL," "RL versus InW, PL," and "RL versus InL, PL," across the selected ranges, the independent variables (PL, PW, InL, and InW) increase from lower to higher values. Initially, the return loss decreases, followed by an increase. The minimum return loss is observed approximately at the center of the surface.

Additionally, for the relationships "F versus PW," "F versus InW," and "F versus InL," within the selected ranges, as the independent variables (PL, PW, InL, and InW) decrease, the resonant frequency increases.

4.3. Optimized antenna results

Numerical optimization. In mobile and wireless technology, a return loss of less than -10 dB is considered the baseline for acceptable performance, with even lower values being ideal, particularly within the frequency range of 28 GHz. To ensure reliable operation, the antenna must be finely tuned to the target frequency. In the numerical optimization method, the goal is set to minimize the return loss (RL) value while ensuring that the parameter F remains within the range of 27.5 GHz to 28.3 GHz. The optimal result obtained from the model is a minimum return loss value of -45.865 dB,

with the following dimensions: PL = 4.7 mm, PW = 4.7 mm, InL = 0.8 mm, and InW = 1 mm.

The antenna's dimensions include the optimized dimensions mentioned above and the fixed dimensions listed in Table 6.

Table 6. Antenna parameters after optimization

Parameter	Dimension (mm)	Parameter	Dimension (mm)
h_g	0.2	PL	4.7
SW	6	h_p	0.2
SL	6	Wf	0.6
h_s	0.2	InL	0.8
PW	4.7	InW	1

The conclusive simulation outcomes validated the precision of the parameter. Figure 3a illustrates how the return loss of the optimized antenna varies with frequency, in comparison to three other antenna structures. The plot reveals that changes in geometric parameters affect both the position of the minimum return loss point and its corresponding value. Additionally, Fig. 3b presents the return loss values, with the optimal value being -45.865 dB at a frequency of 28.122 GHz. As shown in Fig. 3b, the bandwidth (BW) of the antenna is determined by the frequency difference between two junction points at 28.592 GHz and 27.686 GHz, resulting in a bandwidth of 0.906 GHz.

The Voltage Standing Wave Ratio (VSWR) quantifies the power reflected by an antenna. It is recommended that the VSWR value be a positive number. As the VSWR value decreases, the antenna's performance improves, indicating better impedance matching of the transmission line. The ideal VSWR value is 1, which should ideally be below 2 [4]. Fig. 4a shows a visualization of the VSWR for the optimized microstrip patch antenna vs three different designs. Fig. 4b shows that the optimized design has a simulated VSWR of around 1.01.

Figures 5a and 5b depict the optimized antenna's 2D and 3D radiation patterns, respectively. These patterns provide a visual representation of the antenna's performance, illustrating how it radiates and receives energy in space. Fig. 5 highlights the direction in which the antenna exhibits the highest directivity. At a frequency of 28.12 GHz, the antenna attains a peak directivity of 5.58 dBi, with the main beam having an angular width of 51°. The obtained radiation patterns demonstrate good consistency.

Graphical optimization. One key benefit of the DoE method is that it not only identifies the parameters that minimize return loss but also determines the actual return loss value for a specific set of dimensional parameters. This is particularly advantageous because, in practice, if the fabricated dimensions vary within an

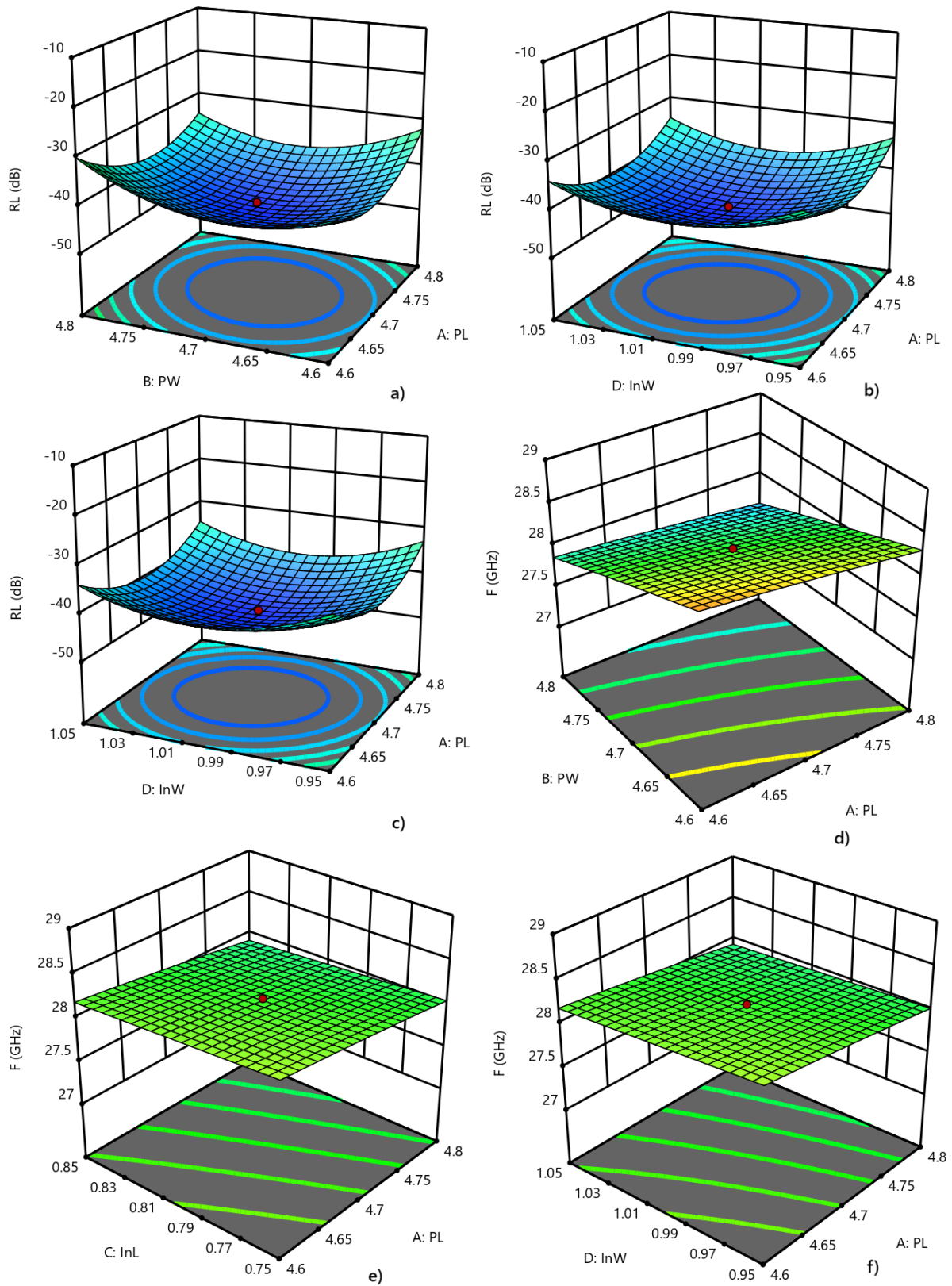


Figure 2. 3D response surfaces of (a) RL versus PW and PL ; (b) RL versus InW and PL; (c) RL versus InL and PL; (d) F versus PW and PL; (e) F versus InL and PL; (f) F versus InW and PL.

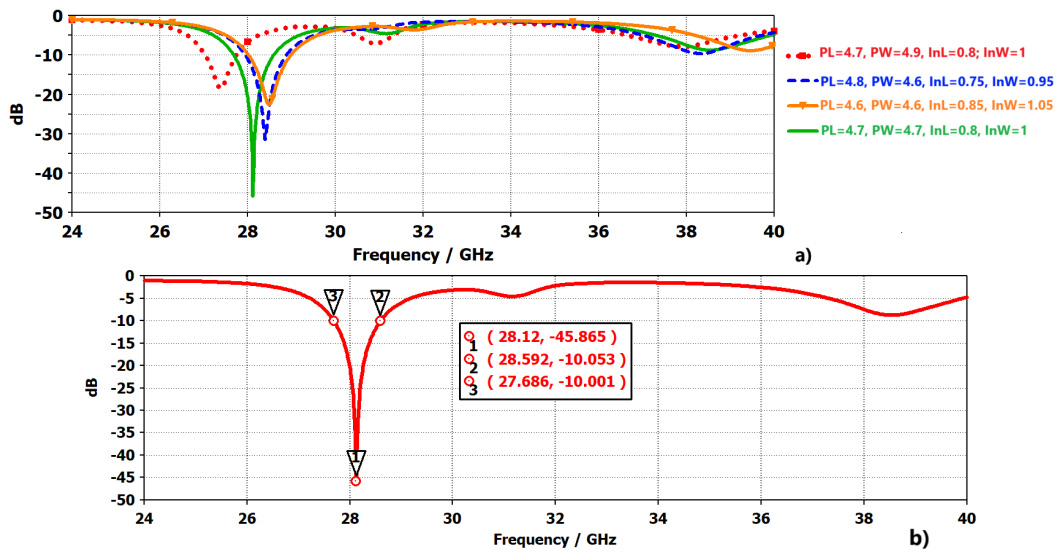


Figure 3. (a) Comparison of the return loss of the optimized antenna with antennas of various sizes; (b) Return loss of the optimized antenna

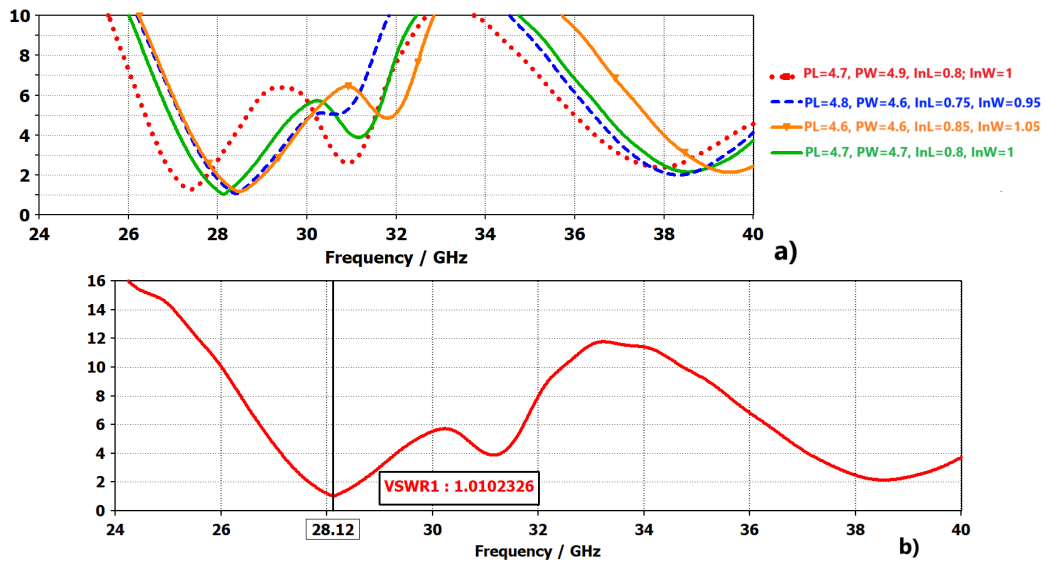


Figure 4. (a) A comparison of the VSWR of the optimized antenna with antennas of various sizes; (b) The VSWR of the optimized antenna

allowable range, the resultant return loss value will be lower than the specified target. This process is known as graphical optimization.

In this method, we establish target response values, specifically the return loss (RL) and the resonant frequency range. This process results in a set of antenna dimensions that satisfy these criteria. For instance, as shown in Fig. 6, with the RL set to -44.5 dB or lower and the F within the range of from 28 to 28.3 GHz, the optimal antenna dimensions fall within the yellow-highlighted area. Specifically, when the values of InW,

InL, PW, and PL vary from InL1 to InL2, InW1 to InW2, PW1 to PW2, and PL1 to PL2, the desired RL and F values are achieved.

The optimized antenna outcomes are compared with earlier publications on dimensions, resonant frequencies, return loss, directivity, VSWR, and bandwidth. As presented in Table 7, the proposed antenna exhibits a return loss (RL) of -45.865 dB, comparable to the -47.7 dB value reported in [28] and approximately 13% lower than that reported in [27]. Notably, this return loss shows an improvement, being lower by a

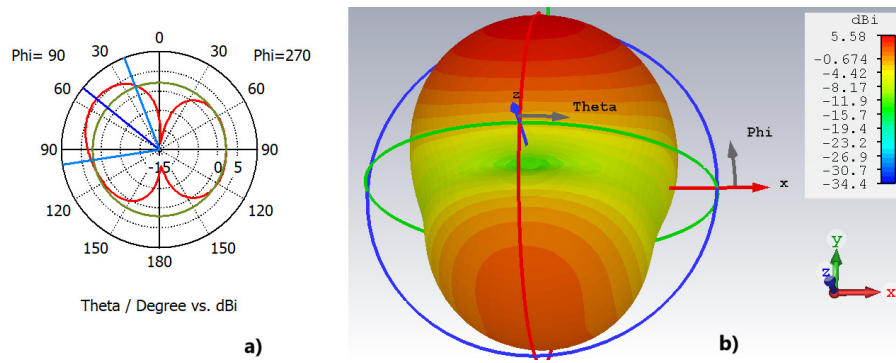


Figure 5. Antenna radiation pattern: (a) 2D and (b) 3D

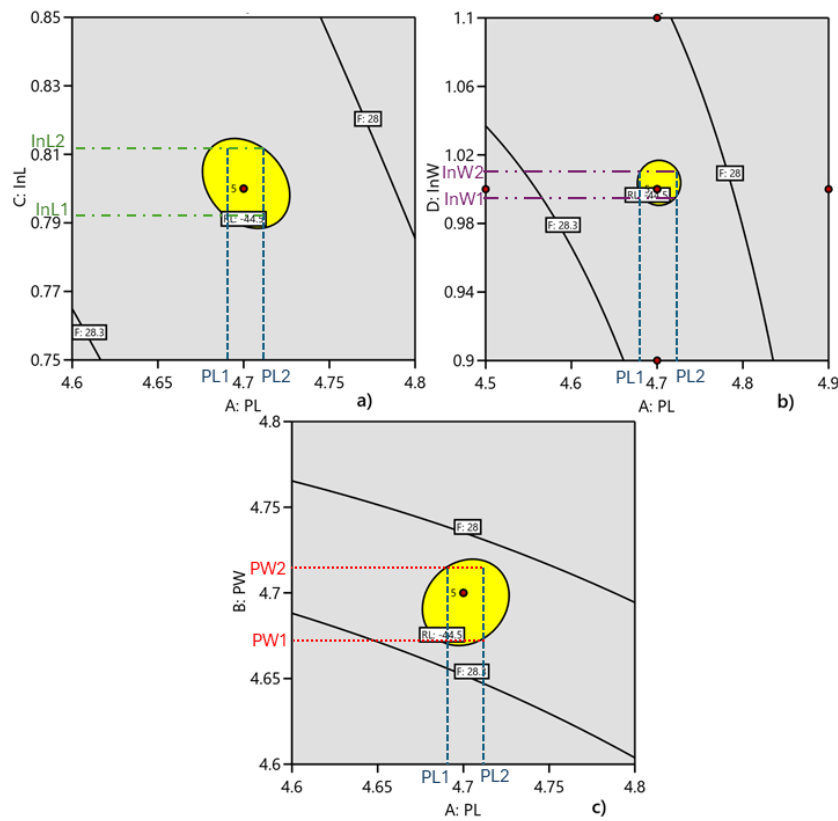


Figure 6. The graphical optimization of the return loss has been set to -44.5 within the frequency range of 28 GHz to 28.3 GHz.

factor of up to 4 compared to other references listed in Table 7, highlighting the enhanced performance of the proposed design. In terms of bandwidth (BW), the designed antenna achieves BW similar to that reported in [22, 25, 26, 33], approximately twice as large as those in [27, 28], but narrower than those presented in [23, 24, 29–32]. It is noteworthy that the designed antenna in this work demonstrates a nearly ideal VSWR value compared to others; however, its limitation lies in having the smallest directivity. As a result, the designed antenna stands out as a strong candidate for 28 GHz

5G applications. The findings indicate that the CCD-RSM optimization method is effective for determining the optimal dimensions of the patch antenna.

5. Conclusions

This paper explores the application of RSM within the framework of DoE to examine the relationship between return loss at the resonant frequency and four input parameters: patch length, patch width, inset slot length, and inset slot width. The investigation focuses on a microstrip patch antenna designed for 5G applications,

Table 7. Comparison results between the optimized antenna and the reference ones.

Reference/year	Dimensions	Frequency (GHz)	RL (dB)	VSWR	Directivity (dB)	BW (GHz)
[22] 2019	$3.4 \times 4.1 \times 0.5$	27.954	-13.48	1.5376	8.37	0.847
[23] 2020	$18 \times 17 \times 1.605$	27.7	-22.2	1.16	6.11	7
[24] 2020	$7 \times 7 \times 0.8$	28	-27.79	1.08	7.45	2.62
[25] 2021	$4.55 \times 4.678 \times 0.15$	27.5	-25.4052	1.095	6.9	0.96
[26] 2022	$4.2 \times 3.3 \times 0.5$	28.008	-17.2	1.32	7.9	0.97
[27] 2022	$3.58 \times 3 \times 0.13$	28	-40.5	-	-	0.51
[28] 2023	$7.24 \times 6.24 \times 0.78$	28	-47.7	-	-	0.482
[29] 2023	$4.2 \times 3.4 \times 0.35$	28	-18.2144	2.1487	6.3094	1.3
[30] 2023	$2.95 \times 2.48 \times 0.35$	28	-24.50	1.12	7.193	1.352
[31] 2024	$6 \times 6 \times 0.254$	28	-35 dB	-	-	19
[32] 2025	$4.3 \times 2.3 \times 0.035$	24.02	-31.54	1.05	8.127	2.8046
[33] 2025	$2.93 \times 2.93 \times 0.25$	28	-35	-	7	1
This work	$4.7 \times 4.7 \times 0.2$	28.122	-45.865	1.01	5.58	0.906

operating within the frequency range of 27.5 GHz to 28.3 GHz. The findings of this study demonstrate that these parameters significantly influence both the return loss and the resonant frequency. Additionally, the study shows that RSM is an effective tool for optimizing return loss at the resonant frequency while analyzing the relationship between the independent and response variables. Using the CCD-RSM experimental model, the optimal result identified was a return loss of -45.865 dB at a resonant frequency of 28.122 GHz. The optimal input parameters were determined to be a patch length of 4.7 mm, a patch width of 4.7 mm, an inset slot length of 0.8 mm, and an inset slot width of 1 mm. The simulated results indicate that the proposed antenna could serve as a strong candidate for wireless communication systems. Future fabrication of the antenna is suggested to compare the actual results with the simulated outcomes.

References

- [1] TUN H.M., LIN Z.T.T., PRADHAN D. and SAHU P.K. (2021). Slotted design of rectangular single/dual feed planar microstrip patch antenna for SISO and MIMO system. In *Proceedings of the 2021 International Conference on Electrical, Computer and Energy Technologies (ICECET)*. 09-10 December 2021; South Africa; IEEE; pp. 1–6. doi: [10.1109/ICECET52533.2021.9698738](https://doi.org/10.1109/ICECET52533.2021.9698738)
- [2] LAVADIYA S.P., SORATHIYA V., KANZARIYA S., CHAVDA B., NAWAED A., FARAGALLAH O.S., EID M.M. and RASHED A.N.Z. (2022). Low profile multiband microstrip patch antenna with frequency reconfigurable feature using pin diode for S, C, X, and Ku band applications. *International journal of communication systems*. 35(9): e5141. doi: [10.1002/dac.5141](https://doi.org/10.1002/dac.5141)
- [3] CHANG L. and LIU H (2021). Low-profile and miniaturized dual-band microstrip patch antenna for 5G mobile terminals. *IEEE Transactions on Antennas and Propagation*. 70(3), pp. 2328–2333. doi: [10.1109/TAP.2021.3118730](https://doi.org/10.1109/TAP.2021.3118730)
- [4] BALANIS C.A. (2016). *Antenna Theory: Analysis and Design*. 4th Edition *John Wiley & sons*.
- [5] KOZIEL S. and OGURTSOV S. (2013). Multi-objective design of antennas using variable fidelity simulations and surrogate models. *IEEE Transactions on Antennas and Propagation*. 61(12): pp. 5931–5939. doi: [10.1109/TAP.2013.2283599](https://doi.org/10.1109/TAP.2013.2283599)
- [6] KUWAHARA Y. (2005). Multiobjective optimization design of Yagi-Uda antenna. *IEEE Transactions on Antennas and Propagation*. 53(6): pp. 1984–1992. doi: [10.1109/TAP.2005.848501](https://doi.org/10.1109/TAP.2005.848501)
- [7] ELIAS B.B.Q., SOH P.J., AL-HADI A.A. and AKKARAEKTHALIN P. (2021). Gain optimization of low-profile textile antennas using CMA and active mode subtraction method. *IEEE Access*. 9: pp. 23691–23704. doi: [10.1109/ACCESS.2021.3056905](https://doi.org/10.1109/ACCESS.2021.3056905)
- [8] KOZIEL S. and BEKASIEWICZ A. (2018). Multi-objective design optimization of antenna structures using sequential domain patching with automated patch size determination. *Engineering Optimization*. 50(2): pp. 218–234. doi: [10.1080/0305215X.2017.1311879](https://doi.org/10.1080/0305215X.2017.1311879)
- [9] AYALEW L.G. and ASMARE F.M. (2022). Design and optimization of pi-slotted dual-band rectangular microstrip patch antenna using surface response methodology for 5G applications. *Heliyon*. 8(12): e12030.
- [10] BEKASIEWICZ A. and KOZIEL S. (2015). Structure and computationally efficient simulation-driven design of compact UWB monopole antenna. *IEEE Antennas and Wireless Propagation Letters*. 14, pp. 1282–1285. doi: [10.1109/LAWP.2015.2402282](https://doi.org/10.1109/LAWP.2015.2402282)
- [11] HAN M., LIU Y., RAKHMANOV R., ISRAEL C., TAJIN M. A. S., FRIEDMAN G. AT EL and GOGOTSI Y. (2021). Solution-processed $Ti_3C_2T_x$ MXene antennas for radio-frequency communication. *Advanced Materials*. 33(1), 2003225. doi: [10.1002/adma.202003225](https://doi.org/10.1002/adma.202003225)
- [12] FERNANDEZ M.D., HERRAIZ D., HERRAIZ D., ALOMANY A. and BELENGUER A. (2022). Design of a wide-bandwidth, high-gain and easy-to-manufacture 2.4 GHz floating patch antenna fed with the through-wire technique. *Applied Sciences*. 12(24): p. 12925. doi: [10.3390/app122412925](https://doi.org/10.3390/app122412925)

- [13] MOHAMED M. Y., DINI A. M., SOLIMAN M. M. and IMRAN A. Z. M. (2020). Design of 2x2 microstrip patch antenna array at 28 GHz for millimeter wave communication. In *Proceedings of 2020 IEEE International Conference on Informatics, IoT, and Enabling Technologies (ICIoT)* 02-05 February 2020; Qatar; IEEE; pp. 445-450. doi: [10.1109/ICIOT48696.2020.9089458](https://doi.org/10.1109/ICIOT48696.2020.9089458)
- [14] GUBRAN M. QUBATI and DIB N. I. (2010). Microstrip patch antenna optimization using modified central force optimization. *Progress In Electromagnetics Research B*. 21(21): pp. 281–298. doi: [10.2528/PIERB10050511](https://doi.org/10.2528/PIERB10050511)
- [15] DOUGLAS C. MONTGOMERY. (2019). Design and Analysis of Experiments *John Wiley & sons* 10th Edition.
- [16] CHEN J.H., CHENG C.Y., CHIEN C.M., YUANGYAI C., CHEN T.H. and CHEN S.T. (2023). Multiple performance optimizations for microstrip patch antenna improvement. *Sensors*. 23(9): p. 4278. doi: [10.3390/s23094278](https://doi.org/10.3390/s23094278)
- [17] AKHTAR F., SALEEM M.M., ZUBAIR M. and AHMAD M. (2023). Design optimization of RF-MEMS based multiband reconfigurable antenna using response surface methodology. In *Proceedings of 2018 Progress in Electromagnetics Research Symposium (PIERS-Toyama)*. 01-04 August 2018; IEEE. pp. 743–750. doi: [10.23919/PIERS.2018.8598186](https://doi.org/10.23919/PIERS.2018.8598186)
- [18] JOSE J., PAULSON A.S.R. and JOSE M.J. (2020). Predicting performance characteristics of double elliptical microstrip patch antenna for radiolocation applications using response surface methodology. *Progress In Electromagnetics Research B*. 88: pp. 35–52. doi: [10.2528/PIERB20051504](https://doi.org/10.2528/PIERB20051504)
- [19] AKDAGLI A. (2007). A closed-form expression for the resonant frequency of rectangular microstrip antennas. *Microwave and Optical Technology Letters*. 49(8): pp. 1848–1852. doi: [10.1002/mop.22572](https://doi.org/10.1002/mop.22572)
- [20] OSKUI F.N., AGHDASINIA H. and SORKHABI M.G. (2019). Modeling and optimization of chromium adsorption onto clay using response surface methodology, artificial neural network, and equilibrium isotherm models. *Environmental Progress & Sustainable Energy*. 38(6): p. 13260. doi: [10.1002/ep.13260](https://doi.org/10.1002/ep.13260)
- [21] MARGARET D.H. and MANIMEGALAI B. (2018). Modeling and optimization of ebg structure using response surface methodology for antenna applications. *AEU-International Journal of Electronics and Communications*. 89, pp. 34–41. doi: [10.1016/j.aeue.2018.03.017](https://doi.org/10.1016/j.aeue.2018.03.017)
- [22] DARBOE O., KONDITI D.B.O. and MANENE F. (2019). A 28 GHz rectangular microstrip patch antenna for 5G applications. *International Journal of Engineering Research and Technology*. 12(6): pp. 854–857.
- [23] JIDNEY M.A., MAHMUD M.Z., RAHMAN M., PAUL L.C. and ISLAM M.T. (2020). A circular shaped microstrip line fed miniaturized patch antenna for 5G applications. In *Proceedings of the 2020 2nd International Conference on Sustainable Technologies for Industry 4.0 (STI)*. 19-20 December 2020; Bangladesh; IEEE. pp. 1–4. doi: [10.1109/STI50764.2020.9350513](https://doi.org/10.1109/STI50764.2020.9350513)
- [24] MERLIN TERESA P. and UMAMAHESWARI G. (2020). Compact slotted microstrip antenna for 5G applications operating at 28 GHz. *IETE Journal of Research*. 68(5): 3778–3785. doi: [10.1080/03772063.2020.1779620](https://doi.org/10.1080/03772063.2020.1779620)
- [25] DIDI S. E., HALKHAMS I., FATTAH M., BALBOUL Y., MAZER S. and BEKKALI M. E. (2021). Design of a microstrip antenna two-slot for fifth generation applications operating at 27.5 GHz. In *International Conference on Digital Technologies and Applications*. Cham: Springer International Publishing. pp. 1081-1089 doi: [10.1007/978-3-030-73882-2](https://doi.org/10.1007/978-3-030-73882-2)
- [26] DIDI S.-E., HALKHAMS I., FATTAH M., BALBOUL Y., MAZER S. and EL BEKKALI M. (2022). Design of a microstrip antenna patch with a rectangular slot for 5G applications operating at 28 GHz. *TELKOMNIKA (Telecommunication Computing Electronics and Control)*. 20(3): pp. 527–536. doi: [10.12928/teikomnika.v20i3.23159](https://doi.org/10.12928/teikomnika.v20i3.23159)
- [27] ALSUDANI A. and MARHOON H.M. (2022). Performance enhancement of microstrip patch antenna based on frequency selective surface substrate for 5G communication applications. *Journal of Communications*. 17 (10): pp. 851–856. doi: [10.12720/jcm.17.10.851-856](https://doi.org/10.12720/jcm.17.10.851-856)
- [28] ALSUDANI A. and MARHOON H.M. (2023). Design and enhancement of microstrip patch antenna utilizing mushroom-like-EBG for 5G communications. *Journal of Communications*. 18(3): pp. 156–163 doi: [10.12720/jcm.18.3.156-163](https://doi.org/10.12720/jcm.18.3.156-163)
- [29] AYOUB S. A., ALSHARBATY F. S. and HAMMODAT A. N. (2023). Design and simulation of high efficiency rectangular microstrip patch antenna using artificial intelligence for 6G era. *TELKOMNIKA (Telecommunication Computing Electronics and Control)* 21(6), pp. 1234-1245. doi: [10.12928/TELKOMNIKA.v21i6.25389](https://doi.org/10.12928/TELKOMNIKA.v21i6.25389)
- [30] RANA M. S., MONIRUZZAMAN M., BISWAS A. N., AZAD T., MONDAL S., ISLAM A. T. U. and SHUVA S. K. S. (2023). Design of 28 GHz Microstrip Patch Antenna for Wireless Applications. *Indonesian Journal of Electrical Engineering and Informatics (IJEEI)*. 11(4), pp. 967-977. doi: [10.52549/ijeei.v11i4.4942](https://doi.org/10.52549/ijeei.v11i4.4942)
- [31] BHADRAVATHI GHOUSE P. S., MANE P. R., ALI T., GOLAPURAM DATTATHREYA G. S., PUTHENVEETIL GOPI S., PATHAN S. and ANGUERA J. (2024). A Low-Profile Circularly Polarized Millimeter-Wave Broadband Antenna Analyzed with a Link Budget for IoT Applications in an Indoor Scenario. *Sensors*. 24(5), 1569. doi: [10.3390/s24051569](https://doi.org/10.3390/s24051569)
- [32] BENKHADDA K., ALTALQI F., BENDALI A., HADDAD A., ZARRIK S., HABIBI S., SAHEL Z., HABIBI M. and HADJOUJDA A. (2025). 1x2 microstrip patch antennas array for mm-waves 5G application. *TELKOMNIKA (Telecommunication Computing Electronics and Control)*. 23(1), pp. 40-47. doi: [10.12928/TELKOMNIKA.v23i1.26263](https://doi.org/10.12928/TELKOMNIKA.v23i1.26263)
- [33] ELSHARKAWY R. R., HUSSEIN K. F. and FARAHAT A. E. (2025). Circularly-polarized 28-GHz antenna for next generations of communication systems. *Scientific Reports*. 15(1), 5745. doi: [10.1038/s41598-025-86236-z](https://doi.org/10.1038/s41598-025-86236-z)